

Bistable mesomorphism and supramolecular stereomutation in chiral liquid crystal azopolymers†

Jesús del Barrio,^a Rosa M. Tejedor,^a Luiz S. Chinelatto,^a Carlos Sánchez,^b Milagros Piñol^a and Luis Oriol^{*a}

Received 22nd January 2009, Accepted 24th April 2009

First published as an Advance Article on the web 4th June 2009

DOI: 10.1039/b901384a

A series of side-chain liquid crystal polymers based on an azobenzene mesogenic unit bearing a terminal chiral chain has been synthesized. The thermal and mesomorphic properties of the homo- and copolymers have been investigated by polarizing optical microscopy, DSC and X-ray diffraction. Polymers having a chiral methylheptyloxy terminal chain (P8S and P8R) exhibit surprising mesomorphic behavior, which depends on the thermal history of the sample. The influence of the molecular chirality and thermal history on the supramolecular organization of the chromophores have also been studied. Supramolecular chiral aggregation of the azobenzenes seems to be responsible for the observed chiroptical properties of these materials, both in solution and solid state (polymeric films), with the handedness controlled by the molecular chirality. Stereomutation of the chiral supramolecular organization is detected when polymeric films of P8S and P8R experience a different thermal history.

Introduction

Chirality in soft matter can be present at two different levels: molecular and supramolecular. Chiral molecules have been widely investigated and are of great interest in several research fields, including pharmacy and biomedicine. Materials chemists have used molecular chirality to produce chiral supramolecular organizations, *e.g.* chiral mesophases.¹ In recent years, the design of new chiral supramolecular materials has received a great deal of attention. For instance, the generation of asymmetry at the supramolecular level starting from achiral molecular precursors is an exciting challenge in Materials Science. Clearly, chirality should appear at the supramolecular level in such achiral compounds. Different physical forces have been studied as sources of supramolecular chirality, *e.g.* breakdown of symmetry in mesophases by vortex motions² or by controlled spinning in spin-coated films.³ Circular polarized light (CPL), as chiral electromagnetic radiation, offers special advantages as a source of chirality and this has been used widely, for instance, to induce absolute asymmetric synthesis.⁴

Transfer of chirality from light to materials requires photoactive groups. In this respect, photochromic polymers have been widely studied and are attractive for many practical applications because of the advantages of stability and processability. Among these polymers, particular attention has been paid to polymers containing azobenzene derivatives, also known as azopolymers.⁵ Applications described for these materials range from optical storage⁵ to photomechanical actuators⁶ derived from the

reversible isomerization of azobenzenes upon irradiation with UV and visible light. Furthermore, liquid crystallinity offers new opportunities for these materials since the cooperative anisotropic interactions of mesogenic azobenzenes can increase the level and stability of the photo-orientation induced in the material.⁷ Within this field, irradiation with CPL of liquid crystalline materials containing azobenzene derivatives may yield supramolecular chiral assemblies with tuned and switchable chiroptical properties. For example, Takezoe and co-workers recently described the selective induction of an enantiomeric excess of a chiral domain in a Bx phase of bent-core molecules by irradiation with CPL (the chirality of the domain depended on the handedness of CPL)⁸ and Sierra and co-workers described columnar propeller-like complexes that have a chiral supramolecular assembly of mesogens, the chirality of which depends on the handedness of CPL.⁹ Nevertheless, most of the studies on the photoinduction of chirality in liquid crystalline materials have been carried out on azopolymers due to the easy preparation of polymeric films and the stability of the induced properties below the T_g. Nikolova and co-workers first reported the photoinduction of chiroptical properties (large circular birefringence and circular dichroism) in films of liquid crystalline side-chain azopolymers.¹⁰ Natansohn, Rochon and co-workers also described photoinduction of chirality in smectic azopolymers and proposed a chiral helical structure whose helicity depends on the polarization of light.¹¹ Nikolova and co-workers also described similar properties in amorphous polymers but in this case prior orientation or irradiation with elliptically polarized light was required.¹² Recently, Cipparrone *et al.* have proposed the photoinduction of a reversible chiral structure, using CPL, in a non-oriented amorphous azopolymer, the structure of which is closely related with mesogenic azopolymers.¹³ We have also described the photoinduction and thermal stability of chiroptical properties in liquid crystalline azopolymers.¹⁴ Based on CD measurements we proposed that the origin of the chiroptical properties in these materials may be attributed to chiral H-aggregates. The supramolecular assembly of azobenzene units in

^aQuímica Orgánica, Facultad de Ciencias-Instituto de Ciencia de Materiales de Aragón, Universidad de Zaragoza-CSIC, Pedro Cerbuna 12, 50009 Zaragoza, Spain

^bDpto. de Física de la Materia Condensada, Facultad de Ciencias-Instituto de Ciencia de Materiales de Aragón, Universidad de Zaragoza-CSIC, Pedro Cerbuna 12, 50009 Zaragoza, Spain

† Electronic supplementary information (ESI) available: Synthesis, characterization and properties of intermediates and polymers. See DOI: 10.1039/b901384a

these aggregates is controlled by the handedness of the CPL used as the chiral stimulus. Transfer of chirality could originate from an asymmetric photoisomerization, which triggers the enrichment of chiral conformations and, consequently, the enrichment of chiral arrangements of azobenzene groups.¹⁵

Nevertheless, less work has been done on chiral azopolymers either in the field of liquid crystal azopolymers or in the study of the supramolecular chirality in this kind of material. For instance, Bobrovsky and co-workers recently reported a comparative study of holographic recording in cholesteric (or chiral nematic) and nematic azobenzene-containing polymers.¹⁶ Kozlovsky and co-workers reported a series of copolymers having an azobenzene unit and a non-photochromic mesogenic unit bearing a chiral terminal chain. In some of these copolymers, complex thermal and mesomorphic behavior was described as they exhibit two smectic phases that depend on the thermal history and, in particular, on the cooling rate from the isotropic state: a proper smectic A phase (SmA) and a phase that appears as isotropic and transparent but with a hidden layered structure of the smectic A type. This phase was designated as an "isotropic smectic phase" and, according to Kozlovsky and co-workers, has a TGBA* structure in which the helical pitch is shorter than the visible wavelength.^{17–19} More recently, the same authors described a homopolymer with an azobenzene containing a chiral terminal chain, which also exhibits a bistable phase behavior (SmA or TGBA*-like phase depending on the cooling rate).^{20,21} The existence of this bistable phase behavior has recently been related to two different isotropic states.²² As far as the influence of irradiation on chiral properties is concerned, Zhang and co-workers described the synthesis and characterization of chiral liquid crystalline azopolymers and studied the CD response before and after irradiation with linearly polarized light.^{23,24} Angiolini *et al.* reported the chiroptical properties of non-liquid crystalline chiral azopolymers, in virgin and irradiated films, both with linear and circular polarized light. It was found that the macromolecular helical suprastructure of these chiral azopolymers was switched by irradiation with circularly polarized light.^{25–28}

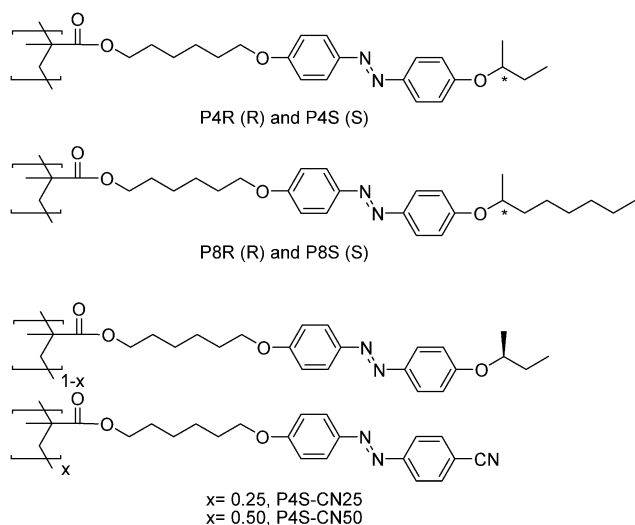


Fig. 1 Chemical structure of the synthesized homo and copolymers (configuration of stereogenic center in brackets).

In this paper we describe the synthesis of a series of azo homopolymers with chiral terminal tails and also copolymers derived from these materials. The structures of these polymers are shown in Fig. 1. Optical, mesomorphic and thermal properties were investigated and, in particular, the influence of the cooling process from the isotropic state on the structure of the resulting mesomorphic glassy state was assessed. The influence of molecular chirality as a chiral trigger for the chiral supramolecular assembly of photochromic units was analyzed both in solution and in polymeric films. The influence of thermal history on the chiroptical properties of polymer films was also analyzed along with the stereomutation of the chiral supramolecular properties by means of the thermal treatment of polymeric films.

Experimental section

Synthesis of monomers

4-Cyano-4'-(6-methacryloyloxyhexyloxy)azobenzene, which was used for copolymerization, was synthesized according to a previously described method.²⁹ Synthesis of chiral monomers is schematically represented in Fig. 2. Synthesis and characterization data for intermediates are collected in the ESI.†

(*R*)-4-Methylpropyloxy-4'-(6''-methacryloyloxyhexyl-1''-oxy)-azobenzene **M4R**. Methacryloyl chloride (0.81 g, 7.74 mmol) was added to a solution of (*R*)-4-methylpropyloxy-4'-(6''-hydroxyhexyl-1''-oxy)azobenzene (1.91 g, 5.16 mmol), triethylamine (1.04 g, 10.30 mmol) and 2, 6-di-*tert*-butyl-4-methylphenol (3 mg) in THF (40.00 mL) under reflux under argon. After 24 h, 10% aqueous NH₄Cl (40 mL) was added. The mixture was extracted with CH₂Cl₂ and the combined organic extracts were washed with water, dried over MgSO₄ and evaporated to dryness. The crude product was purified by flash chromatography eluting with hexane/ethyl acetate (10:1) to yield the pure monomer as a yellow solid. Finally, the product was recrystallized from absolute ethanol. Yield: 76%. ¹H NMR (400 MHz, CDCl₃, δ): 7.86 (dd, *J* = 9.0 Hz, *J* = 2.1 Hz, 4H), 6.96 (dd, *J* = 9.0 Hz, *J* = 1.9 Hz, 4H), 6.08 (s, 1H), 5.51 (s, 1H), 4.40–4.29 (m, 1H), 4.13 (t, *J* = 6.5 Hz, 2H), 3.94 (t, *J* = 6.5 Hz, 2H), 1.92 (s, 3H), 1.89–1.35 (m, 10H), 1.32 (d, *J* = 6.1 Hz, 3H), 0.99 (t, *J* = 7.5 Hz, 3H). ¹³C NMR (100 MHz, CDCl₃, δ): 167.39, 161.05, 160.38, 146.90, 146.71, 136.52, 124.98, 124.34, 124.25, 115.71, 114.56, 75.19, 68.09, 64.64, 32.60, 29.12, 29.08, 25.81, 25.50, 19.16, 18.36, 9.70. IR (KBr, cm⁻¹): 2969, 2939, 2868, 1702, 1601, 1581, 1500, 1240, 1151, 840. Anal. Found (calcd): C 71.12% (71.21), H 7.83% (7.81), N 6.34% (6.39).

(*S*)-4-Methylpropyloxy-4'-(6''-methacryloyloxyhexyl-1''-oxy)-azobenzene **M4S**. Prepared from **7(S)** according to the procedure described for **M4R**. Yellow solid (72% yield). ¹H NMR (400 MHz, CDCl₃, δ): 7.85 (dd, *J* = 9.0 Hz, *J* = 2.1 Hz, 4H), 6.96 (dd, *J* = 9.0 Hz, *J* = 1.9 Hz, 4H), 6.08 (s, 1H), 5.51 (s, 1H), 4.38–4.29 (m, 1H), 4.13 (t, *J* = 6.5 Hz, 2H), 3.94 (t, *J* = 6.5 Hz, 2H), 1.92 (s, 3H), 1.89–1.35 (m, 10H), 1.33 (d, *J* = 6.1 Hz, 3H), 0.99 (t, *J* = 7.5 Hz, 3H). ¹³C NMR (100 MHz, CDCl₃, δ): 167.41, 161.05, 160.38, 146.91, 146.71, 136.52, 125.26, 124.34, 124.24, 115.71, 114.56, 75.19, 68.08, 64.64, 32.60, 29.12, 29.08, 25.81, 25.50, 19.16, 18.36, 9.70. IR (KBr, cm⁻¹): 2968, 2939, 2868, 1703, 1601, 1581, 1500, 1240, 1151, 840. Anal. Found (calcd): C 71.18% (71.21), H 7.80% (7.81), N 6.45% (6.39).

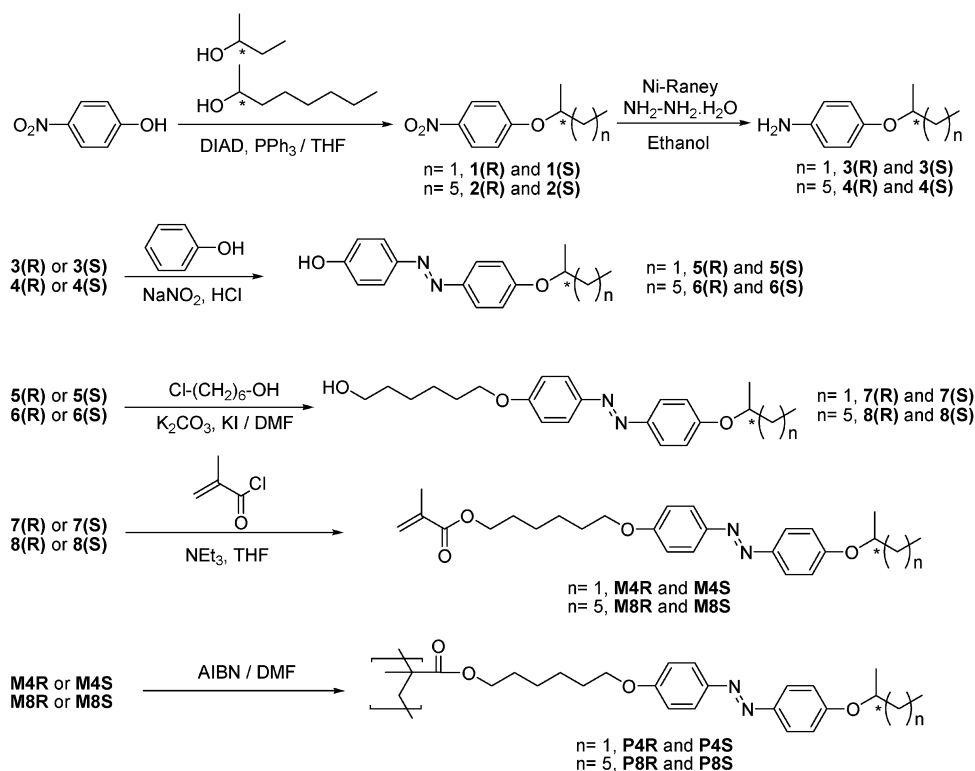


Fig. 2 Chemical structure of the synthesized homo and copolymers.

(*R*)-4-Methylheptyloxy-4'-(6''-methacryloylxyhexyl-1''-oxy)-azobenzene **M8R**. Prepared from **8(R)** according to the procedure described for **M4R**. Yellow solid (77% yield). $^1\text{H NMR}$ (400 MHz, CDCl_3 , δ): 7.86 (dd, $J = 9.0$ Hz, $J = 2.9$ Hz, 4H), 6.97 (dd, $J = 9.0$ Hz, $J = 4.8$ Hz, 4H), 6.10 (s, 1H), 5.55 (s, 1H), 4.49–4.40 (m, 1H), 4.17 (t, $J = 6.6$ Hz, 2H), 4.04 (t, $J = 6.4$ Hz, 2H), 1.95 (s, 3H), 1.88–1.23 (m, 21H), 0.88 (t, $J = 6.9$ Hz, 3H). $^{13}\text{C NMR}$ (100 MHz, CDCl_3 , δ): 167.52, 161.01, 160.35, 146.98, 146.76, 136.48, 125.22, 124.32, 124.26, 115.76, 114.62, 74.18, 68.07, 64.62, 36.41, 31.77, 29.25, 29.10, 28.56, 25.80, 25.74, 25.47, 22.59, 19.72, 18.33, 14.07. IR (KBr, cm^{-1}): 2970, 2942, 2868, 1701, 1600, 1637, 1581, 1502, 1240, 1151, 843. Anal. Found (calcd): C 72.66% (72.84), H 8.60% (8.56), N 5.60% (5.66).

(*S*)-4-Methylheptyloxy-4'-(6''-methacryloylxyhexyl-1''-oxy)-azobenzene **M8S**. Prepared from **8(S)** according to the procedure described for **M4R**. Yellow solid (72% yield). $^1\text{H NMR}$ (400 MHz, CDCl_3 , δ): 7.86 (dd, $J = 9.0$ Hz, $J = 2.9$ Hz, 4H), 6.97 (dd, $J = 9.0$ Hz, $J = 4.8$ Hz, 4H), 6.10 (s, 1H), 5.55 (s, 1H), 4.50–4.40 (m, 1H), 4.17 (t, $J = 6.6$ Hz, 2H), 4.04 (t, $J = 6.4$ Hz, 2H), 1.95 (s, 3H), 1.88–1.22 (m, 21H), 0.88 (t, $J = 6.9$ Hz, 3H). $^{13}\text{C NMR}$ (100 MHz, CDCl_3 , δ): 167.29, 161.06, 160.40, 146.85, 146.64, 136.48, 125.23, 124.38, 124.31, 115.77, 114.63, 74.19, 68.07, 64.62, 36.40, 31.77, 29.25, 29.10, 28.55, 25.80, 25.74, 25.47, 22.59, 19.72, 18.33, 14.07. IR (KBr, cm^{-1}): 2970, 2940, 2868, 1701, 1636, 1599, 1581, 1502, 1240, 1151, 843. Anal. Found (calcd): C 72.70% (72.84), H 8.58% (8.56), N 5.72% (5.66).

Synthesis of polymers

Polymers and copolymers were prepared according to a standard method: the corresponding monomer (or mixture of monomers)

was dissolved in freshly distilled DMF (approximately 10% w/v) under an argon atmosphere in a Schlenk tube. The sample was degassed by several vacuum/argon cycles, the solution was heated at 70 °C and azobis(isobutyronitrile) (AIBN) (1% weight ratio) was added. The solution was stirred at this temperature for 48 h and the progress of the polymerization was monitored by thin layer chromatography. The polymer was precipitated by pouring the reaction mixture into in cold 96% ethanol and the product was filtered off. Purification of the polymer was carried out by Soxhlet extraction with ethanol for 48 h. The final products were obtained as yellow powders and were dried at 50 °C under vacuum to constant weight (determined by thermogravimetry).

P4R. Yellow powder (71% yield). $^1\text{H NMR}$ (400 MHz, CDCl_3 , δ): 7.88–7.76 (m, 4H), 7.01–6.84 (m, 4H), 4.43–4.28 (m, 1H), 4.06–3.82 (m, 4H), 2.00–1.17 (m, 16H), 1.14–0.78 (m, 5H). $^{13}\text{C NMR}$ (100 MHz, CDCl_3 , δ): 177.76–176.89, 161.09, 160.40, 147.09, 146.95, 124.32, 124.29, 115.89, 114.70, 75.36, 68.15, 65.01, 54.30, 45.31–45.03, 30.25, 29.16, 27.31, 25.92, 25.74, 19.18, 18.76–16.84, 9.77. IR (KBr, cm^{-1}): 2974, 2935, 2860, 1727, 1599, 1580, 1499, 1452, 1246, 1146, 840. Anal. Found (calcd): C 71.04% (71.21), H 7.87% (7.81), N 6.32% (6.39). $[\alpha]_D = -16.3$ (c 1.19, CHCl_3). GPC (THF, PMMA standards): $M_n = 24000$, $M_w = 36200$, IP = 1.5.

P4S. Yellow powder (56% yield). $^1\text{H NMR}$ (400 MHz, CDCl_3 , δ): 7.90–7.75 (m, 4H), 7.01–6.82 (m, 4H), 4.40–4.25 (m, 1H), 4.06–3.80 (m, 4H), 2.01–1.22 (m, 16H), 1.10–0.83 (m, 5H). $^{13}\text{C NMR}$ (100 MHz, CDCl_3 , δ): 177.84–176.84, 161.08, 160.35, 146.96, 146.79, 124.41, 124.37, 115.80, 114.64, 75.25, 68.09, 65.02, 54.30 45.23–44.91, 30.29, 29.18, 27.35, 25.98, 25.81, 19.25,

18.75–16.85, 9.79. IR (KBr, cm^{-1}): 2975, 2931, 2857, 1726, 1599, 1580, 1500, 1452, 1247, 1146, 839. Anal. Found (calcd): C 70.94% (71.21), H 7.79% (7.81), N 6.31% (6.39). $[\alpha]_{\text{D}} = +19.0$ (c 1.00, CHCl_3). GPC (THF, PMMA standards): $M_n = 23700$, $M_w = 34300$, $IP = 1.4$.

P8R. Yellow powder (76% yield). ^1H NMR (400 MHz, CDCl_3 , δ): 7.88–7.70 (m, 4H), 7.00–6.79 (m, 4H), 4.46–4.28 (m, 1H), 4.10–3.74 (m, 4H), 1.85–0.98 (m, 26H), 0.97–0.74 (m, 3H). ^{13}C NMR (100 MHz, CDCl_3 , δ): 177.49–176.56, 161.03, 160.29, 146.90, 146.71, 124.37, 124.32, 115.72, 114.58, 74.10, 68.10, 65.15–64.91, 54.60, 45.19–44.70, 36.40, 31.76, 29.30, 29.20, 28.13, 25.96, 25.79, 25.43, 22.58, 19.70, 18.76–16.84, 14.07. IR (KBr, cm^{-1}): 2975, 2924, 2857, 1726, 1598, 1578, 1499, 1450, 1250, 1141, 842. Anal. Found (calcd): C 72.62% (72.84), H 8.60% (8.56), N 5.72% (5.66). $[\alpha]_{\text{D}} = +9.5$ (c 1.12, CHCl_3). GPC (THF, PMMA standards): $M_n = 36100$, $M_w = 57300$, $IP = 1.6$.

P8S. Yellow powder (72% yield). ^1H NMR (400 MHz, CDCl_3 , δ): 7.94–7.77 (m, 4H), 7.01–6.81 (m, 4H), 4.48–4.27 (m, 1H), 4.09–3.73 (m, 4H), 1.85–0.97 (m, 26H), 0.93–0.77 (m, 3H). ^{13}C NMR (100 MHz, CDCl_3 , δ): 177.77–176.66, 161.26, 160.59, 146.40, 146.24, 124.65, 124.53, 115.80, 114.67, 74.20, 68.12, 65.08–64.87, 54.63, 45.19–44.70, 36.43, 31.81, 29.29, 29.15, 28.11, 25.96, 25.78, 25.47, 22.62, 19.70, 18.78–16.86, 14.11. IR (KBr, cm^{-1}): 2976, 2925, 2856, 1727, 1600, 1578, 1500, 1453, 1251, 1139, 840. Anal. Found (calcd): C 72.70% (72.84), H 8.60% (8.56), N 5.74% (5.66). $[\alpha]_{\text{D}} = -10.5$ (c 1.04, CHCl_3). GPC (THF, PMMA standards): $M_n = 37700$, $M_w = 67500$, $IP = 1.8$.

P4S-CN50. The molar composition of the feed in this case was 50% of 4-cyano-4'-(6-methacryloyloxyhexyloxy)azobenzene and 50% of **M4S**. Orange powder (40% yield). ^1H NMR (400 MHz, CDCl_3 , δ): 7.95–7.64 (m, 10H), 7.00–6.82 (m, 6H), 4.40–4.27 (m, 1H), 4.07–3.81 (m, 8H), 2.00–0.78 (m, 34H). ^{13}C NMR (100 MHz, CDCl_3 , δ): 177.46–176.34, 162.50, 162.34, 160.32, 154.56, 146.85, 146.72, 146.60, 133.05, 125.43, 124.33, 124.28, 124.03, 123.03, 118.58, 115.71, 114.72, 114.52, 75.20, 68.16, 67.98, 65.03–64.82, 53.21–52.12, 45.23–44.82, 30.30, 29.09, 28.16, 28.05, 28.01, 25.91, 25.84, 25.74, 25.30, 19.17, 18.71–16.34, 9.73. IR (KBr, cm^{-1}): 2975, 2926, 2855, 2225, 1726, 1599, 1580, 1499, 1451, 1250, 1140, 842. Anal. Found (calcd): C% 70.68 (70.89), H% 6.95 (7.12), N% 8.70 (8.56). GPC (THF, PMMA standards): $M_n = 8800$, $M_w = 10200$, $IP = 1.2$.

P4S-CN25. In this case, the molar composition of the feed was 25% of 4-cyano-4'-(6-methacryloyloxyhexyloxy)azobenzene and 75% of **M4S**. Orange powder (45% yield). ^1H NMR (400 MHz, CDCl_3 , δ): 7.95–7.63 (m, 9H), 7.03–6.82 (m, 7H), 4.43–4.27 (m, 1.5H), 4.09–3.80 (m, 8H), 1.98–0.77 (m, 38H). ^{13}C NMR (100 MHz, CDCl_3 , δ): 177.46–176.01, 162.42, 162.30, 160.45, 154.57, 146.95, 146.74, 146.58, 133.05, 125.41, 124.27, 124.25, 123.98, 123.03, 118.61, 115.67, 114.70, 114.52, 75.21, 68.21, 68.02, 65.10–64.87, 53.19–52.03, 45.25–44.79, 30.26, 29.11, 28.16, 28.06, 27.96, 25.87, 25.82, 25.73, 25.29, 19.15, 18.75–16.31, 9.70. IR (KBr, cm^{-1}): 2976, 2936, 2859, 2225, 1726, 1598, 1580, 1499, 1450, 1248, 1145, 841. Anal. Found (calcd): C% 70.96 (71.05), H% 7.38 (7.47), N% 7.51 (7.48). GPC (THF, PMMA standards): $M_n = 10400$, $M_w = 11600$, $IP = 1.1$.

The molar compositions of the copolymers were determined from ^1H NMR spectra by comparing the integrated areas of the signals at 4.35 and 3.95 ppm. The molar contents of the copolymers reflect the feed composition, indicating similar reactivities of the two monomers.

General procedures

Elemental analyses were performed using a Perkin-Elmer 240C microanalyzer. IR spectra were obtained on a Nicolet Avatar 360-FTIR using KBr discs. ^1H NMR spectra were measured at room temperature with a Bruker AV-4 spectrometer. Molecular weights of polymers were determined by GPC using a Waters 2695 autosampler equipped with two in line Waters HR-4 and HR-2 columns and a Waters 2420 ELSD detector, using THF as the eluent at 35 °C and calibrated with polystyrene narrow standards. Measurements were performed in THF at room temperature with 1 mL/min flow, using PMMA narrow molecular weight standards. UV-Vis spectra were recorded with a UV-Vis spectrophotometer UV4-200 from ATI-Unicam. Optical rotations were measured at room temperature on chloroform solutions (concentrations are given in g/100 mL) on a JASCO P-1020 polarimeter, using a quartz cell with 1 cm optical path length. CD spectra were registered using a Jasco J-810 spectropolarimeter by using either polymer solutions of polymer films. The CD spectra of the films were registered by rotating the samples every 60 degrees around the light beam axis. In the case of polymer solutions (see below) dichloromethane (DCM) or DCM/hexane were used as solvents. DCM is a good solvent for the polymers and transparent polymer solutions were easily obtained in all cases. In the case of hexane solutions, the polymers were first dissolved in the minimum amount of hot DCM and warm hexane was added up to the required concentration. Fresh and transparent solutions were only obtained in the case of polymers having the longest terminal aliphatic chain and measurements were made at room temperature (rt). Both in DCM and DCM/hexane solutions the concentration was maintained at around 4×10^{-2} mg/mL. The polymer films were obtained by casting from DCM solutions onto fused silica plates. Thermogravimetric analyses (TGA) were performed using a TA Q-5000 instrument at a heating rate of 10 °C min^{-1} under a nitrogen atmosphere. Mesogenic behavior was evaluated by polarized-light optical microscopy (POM) using an Olympus BH-2 polarizing microscope fitted with a Linkam THMS600 hot stage and a CSI96 cooling system and operating at different scan rates in order to evaluate the influence of thermal history on the liquid crystalline textures. Thermal transitions were determined by differential scanning calorimetry (DSC) using a TA DSC Q-2000 instrument under a nitrogen atmosphere. Glass transition temperatures (T_g) were determined at the midpoint of the baseline jump and the mesophase-isotropic phase transition temperature was read at the maximum of the corresponding peaks using powdered samples of about 4–6 mg. XRD measurements of polymeric samples were performed with an evacuated Pinhole camera (Anton-Paar) operating with a point-focused Ni-filtered $\text{Cu-K}\alpha$ beam. Samples were held in Lindemann glass capillaries and the patterns were collected on flat photographic films perpendicular to the X-ray beam.

Results and discussion

Synthesis and characterization

The synthetic pathway to the target polymers is represented in Fig. 2. Chiral terminal chains were introduced by etherification of *p*-nitrophenol using a Mitsunobu reaction. Subsequent reduction of the nitro group and azo-coupling of the derived aniline with phenol gave rise to the desired azochromophores. A flexible spacer was introduced by a Williamson reaction and finally the methacroyl group was incorporated by esterification with methacroyl chloride. Polymers were synthesized by a conventional free-radical polymerization using AIBN as a thermal initiator and DMF as the solvent. Average molecular weights and polydispersities (of final purified samples) were analyzed by GPC using PMMA standards as references. The results are gathered in Table 1. The incorporation of cyanoazobenzene comonomer leads to a small decrease in the molecular weight. Chemical structures were corroborated by elemental analysis, NMR and spectroscopic methods (see Experimental Part). A detailed analysis of the ^{13}C NMR spectra (see ESI†) provided evidence that the polymer chain has a tendency to syndiotacticity, as widely reported for polymethacrylates under similar conditions.³⁰

Thermal and mesomorphic properties

The thermal stability of the target polymers was studied by thermogravimetry (see Table 1) using powdered samples. All of the studied polymers exhibit good thermal stability up to approximately 270 °C, with the onset of decomposition detected at temperatures above 300 °C. Mesomorphic properties were analyzed by POM, DSC and X-ray diffraction and the results are summarized in Table 1. Polymers with the shortest terminal chain (P4R and P4S) seem to be amorphous according to the DSC results. Thus, as can be observed in the second heating scans corresponding to these polymers (Fig. 3), a glass transition is detected for both polymers but in case of P4S a small endotherm can be more clearly seen in the final region of the glass transition, which in principle might be associated to enthalpy

Table 1 Thermal and mesomorphic properties of the synthesized azo-polymers

Polymer	Mn/IP ^a	T _{1%} /T _{ONSET} ^b	Thermal transition ^c
P4R	24000/1.5	287/317	g 40 I ^d
P4S	23700/1.4	283/328	g 51 SmA 66 I ^e
P4S-CN25	10400/1.1	387/330	g 49 SmA 94 (8.7) I
P4S-CN50	8800/1.2	270/317	g 51 SmA 109 (6.8) I
P8R	36100/1.6	294/346	g 50 SmA 78 (6.8) I ^f
P8S	37700/1.8	306/344	g 49 SmA 76 (6.3) I ^f

^a Mn, weight average molecular mass; IP, polydispersity. ^b (°C) Decomposition detected in the derivative thermogravimetric curve; T_{1%}: temperature corresponding to 1% weight loss; T_{ONSET}: onset of the decomposition peak. ^c Transition temperatures are indicated in °C and enthalpy (in brackets) in J/g and correspond to the second heating scan (scan rate: 10 °C/min). ^d Endotherm transition (mesophase-isotropic, see text) overlapped with glass transition. Enthalpy cannot be accurately calculated. ^e Please see text for the discussion about the dependence of the mesomorphic behaviour on the thermal history. ^f Glass transition was calculated in virgin samples.

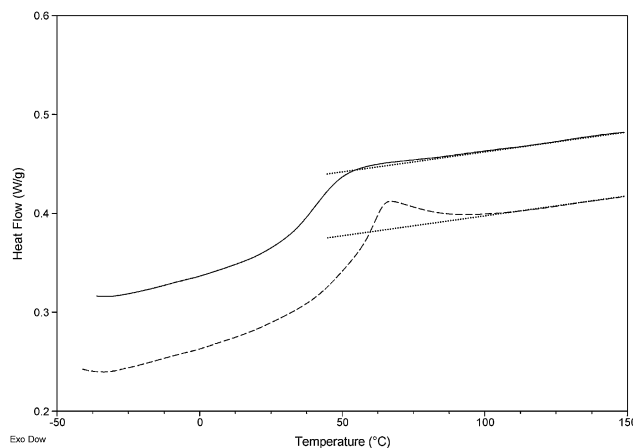


Fig. 3 DSC traces corresponding to the second heating scans (10 °C/min) of P4R (up) and P4S (down).

relaxation. However, a small exotherm overlapping the glass transition is also observed in the cooling process from the isotropic state, which seems more likely to point to a phase transition and could be related to an isotropic-mesophase transition. In fact, when the homopolymers P4R and P4S were carefully studied under the polarizing optical microscope, a very poorly defined grainy texture was detected on cooling from the isotropic state. This result points to a short range mesophase that in the case of P4R overlaps with the glass transition and, consequently, only gives rise to a baseline jump. In order to corroborate this mesomorphic behavior, samples with different thermal histories were studied by X-ray diffraction. When samples were cooled from approximately 100 °C to rt at cooling rates of about 10 °C/min, X-ray diffraction patterns only showed a diffuse and broad scattering peak at high angles, which roughly corresponds to a distance of 4.5 Å (related to the typical intermolecular distance of mesogenic units). However, when the samples were annealed at temperatures just above the glass transition (at around 55–60 °C) and finally cooled to rt, a new and relatively sharp scattering peak was clearly detected at low angles. This new peak was detected after 5 h of annealing for P4S, although longer annealing times (higher than 20 h) were needed to observe a similar peak in the case of P4R. The appearance of this peak can be associated with a lamellar phase with a measured layer spacing of 28.5 Å. The molecular length of the repeating unit of the azobenzene chromophores with methylpropyl terminal chains is 28 Å as estimated using Dreiding stereomodels with a fully extended conformation. This finding could be indicative of a SmA phase with a monolayer structure.

Copolymers P4S-CN25 and P4S-CN50 combine this chiral photochromic unit and the well-known smectogen 4-cyanoazobenzene. Mesomorphism was clearly observed for these copolymers. Thus, when P4S-CN25 was cooled down from the isotropic state, a turbid, polydomain mesomorphic phase was obtained with a poorly defined, grainy texture. In the case of P4S-CN50, typical fan-shaped and homeotropic textures of a SmA phase were clearly detected. DSC traces of these polymers show a glass transition and an endothermic peak corresponding to the isotropization detected by optical microscopy. X-Ray diffraction measurements also confirmed the SmA nature of the mesophase

of both copolymers, with a monolayer structure with a measured layer thickness of about 29 Å. In the case of P4S-CN50 a well-oriented fiber could be obtained directly from the mesophase and its diffractogram confirms the orthogonal arrangement of the mesogenic units in the smectic phase.

In an attempt to obtain chiral azo homopolymers with a broader range of mesomorphism, a longer terminal chain (P8R and P8S) was introduced but with the stereogenic center maintained in the same position, *i.e.* adjacent to the aromatic core. DSC traces of azopolymers containing 1-methylheptyl chiral terminal chains (P8R and P8S) exhibit a peak both in the heating and cooling processes and these correspond to the mesophase-isotropic phase transition according to POM observations (see below). The glass transition is only clearly detected in the first heating scan, as can be seen in Fig. 4, which represents the first heating and cooling scan as well as the second heating scan. However, the glass transition is hardly detected on cooling or on successive scans.

The nature of the mesomorphic phase of these azopolymers was studied by POM and X-ray diffraction. Firstly, it must be pointed out that mesomorphic textures and the transmission of films of chiral homopolymers P8R and P8S are strongly affected by thermal history. Thus, when the polymers were slowly cooled down in the absence of light from the isotropic state (at cooling rates lower than 3 °C/min) a birefringent, very poorly defined sanded texture was observed and the sample appeared turbid by the naked eye (Fig. 5a). However, on cooling at rates higher than 5 °C/min the sample was more transparent and dark textures were detected by POM (Fig. 5b). These observations point to kinetic and thermodynamic control of the mesomorphic organization of these materials.

Samples with a different thermal history were also studied by DSC in order to investigate the influence of the cooling process on the phase transitions of the resulting mesomorphic glasses. In fact, the study of the mesophase-isotropic phase transition, as well as the enthalpy of mesomorphic glasses obtained under different cooling conditions, provided some evidence of a thermal history-dependent mesomorphic organization. As an

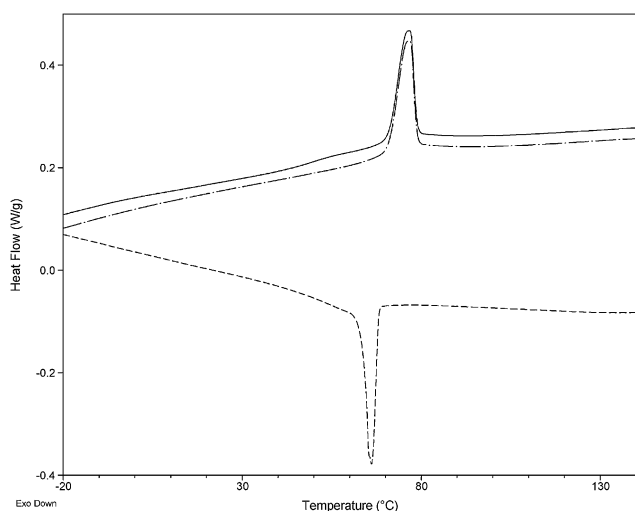


Fig. 4 DSC traces corresponding to first heating scan (up), first cooling scan (down) and second heating scan (middle) of P8S (10 °C/min).



Fig. 5 Microphotographs taken at room temperature of a sample of P8S cooled from the isotropic state at 1 °C/min (a) and 20 °C/min (b). Insets: photographs of a sample of P8S cooled at 1 °C/min (translucent sample, a) or 20 °C/min (transparent sample, b).

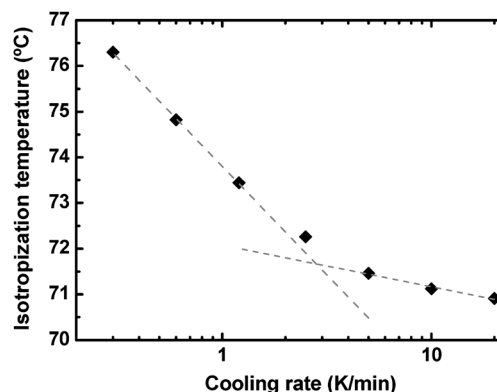


Fig. 6 Dependence of the isotropization rate temperature of a sample of P8S cooled at different rates from the isotropic state (isotropization temperature was measured on heating at 10 °C/min).

example, the variation of the isotropization temperature measured in the heating scan (fixed heating rate 10 °C/min) of a sample of P8S previously cooled down from the isotropic state to the mesomorphic glass state at different cooling rates is represented in Fig. 6. As can be seen, the isotropization temperature varies linearly with the cooling rate, but there are two different regimes, with the change of slope of this dependence located at around 3 °C/min. This behavior is similar to the phase transition behavior of bistable crystallizable polymers.³¹ In the field of liquid crystalline polymers, this behavior has been assigned in similar azopolymers to the existence of a bistable mesomorphism and, consequently, to the appearance of two different mesophases depending on the thermal history.³²

The nature of the mesophase of polymers P8R and P8S was also studied by X-ray diffraction (see ESI†). Samples of these polymers were cooled down from the isotropic state up to rt at different cooling rates and finally studied at rt (mesomorphic glass). All of the materials (even quenched samples) exhibit typical X-ray diffraction patterns compatible with a smectic phase, with a peak at low angles corresponding to a layer spacing of about 54.8 Å (the molecular length of the monomeric unit is 33 Å, as estimated with Dreiding stereomodels for a fully extended conformation). Significant differences were not observed in the layer thickness for samples cooled at different cooling rates and only a more reinforced peak at low angle was detected for samples cooled at low cooling rates. Furthermore, the layer thickness did not vary with the temperature. These facts point to

an orthogonal smectic A mesophase that has a bilayer structure with interdigitation of the terminal chains.

Bearing these results in mind, the mesophase obtained by slow cooling (slower than 3 °C/min) can be assigned as a SmA phase. Furthermore, the phase obtained by a fast cooling process must be structurally related with an orthogonal layered phase according to the X-ray diffraction data. Small domains of SmA phase might partially explain these results, however, as mentioned above, Kozlovski and co-workers previously described similar bistable mesomorphic behavior in chiral homo- and co-azopolymers having a similar chemical structure. They described a “transparent mesophase”³³ with a hidden layered structure obtained by fast cooling, which was assigned to a TGBA* mesophase, *i.e.* smectic A domains rotated in a regular way to form a helical superstructure.³⁴ According to these authors the bistable mesomorphism of P8R and P8S may be tentatively assigned to SmA or TGBA* phases, and these phases have a thermodynamic or kinetic control imposed by the thermal history.

Supramolecular chirality

As reported previously, circular polarized light (CPL) can be used as a chiral stimulus to generate asymmetry in liquid crystals.³⁵ Indeed, CPL is capable of photoinducing chiral aggregation of azobenzene chromophores of side-chain liquid crystalline azopolymers.¹⁴ In this respect, we recently proposed that supramolecular chiral aggregation could begin at the molecular level with an asymmetric chemical modification photoinduced by CPL.¹⁵ In a similar way, molecular chirality can induce a chiral aggregation of azobenzene units and give rise to a chiral azo-material that combines molecular and supramolecular chirality. In order to assess the formation of chiral aggregation due to molecular chirality, solutions of the synthesized chiral homopolymers were prepared both in DCM and DCM/hexane mixtures in order to study the relationship between the solvent polarity and the aggregation of azobenzene moieties. Unfortunately, P4R and P4S precipitate on adding even a small amount of hexane and, consequently, these studies were only carried out with P8S and P8R using fresh samples (eventually a partial precipitation of the polymers was observed on storing the solutions for several days).

UV-Vis and circular dichroism (CD) spectra of P8S and P8R in DCM and DCM/hexane mixtures are gathered in Fig. 7. The UV-Vis spectrum of P8S in DCM solution (or P8R, see ESI†) is similar to the spectrum of the monomer and exhibits a strong π - π^* transition at 362 nm and a weak n - π^* transition at around 450 nm, as corresponds to *E*-azobenzene chromophores. Taking into account that DCM is a good solvent for P8S and P8R, along with the symmetry of the main band of the absorption spectrum (the band is very similar to the exhibited by low concentrated monomeric solutions), it can be concluded that the chromophores are essentially isolated. The UV-Vis spectra of P8S and P8R in a low polarity solvent such as DCM/hexane mixtures (minimum amount of DCM) display a significant blue shift of the π - π^* transition compared to those exhibited by homopolymers in DCM solutions (crossover from 362 to 342 nm). This blue shift is associated with the formation of H-aggregates³⁶ as a consequence of the low interaction of azochromophores with the non-

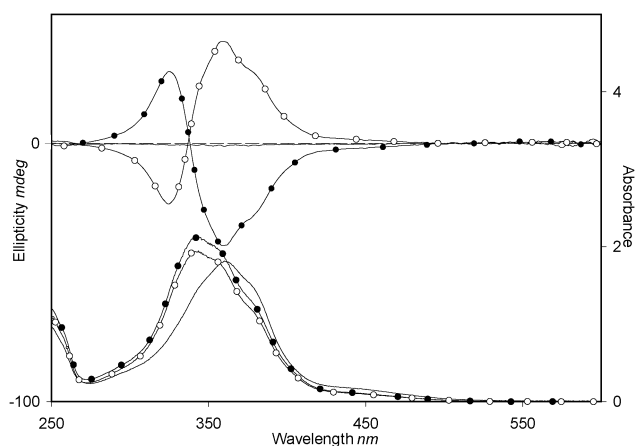


Fig. 7 UV-vis (down) and CD spectra (up) of P8S in DCM solution (—), and P8S and P8R in DCM/hexane solution (—●—) and (---) respectively.

polar solvent, which forces non-covalent interactions between the azo units and results in a supramolecular arrangement.

The DCM solutions of P8S (Fig. 7) and P8R (ESI) are CD-silent. However, these polymers in DCM/hexane solutions exhibit significant CD signals of opposite sign: the spectrum of P8S displays a band that can be associated to a negative exciton couplet while P8R exhibits the inverted band corresponding to a positive couplet. Angiolini *et al.* studied amorphous chiral azopolymethacrylates with a chiral spacer between the main chain and the azobenzene units, which was consequently close to the methacrylate group.^{26,37,38} These materials exhibit similar CD responses in different organic solvents, *e.g.* CHCl₃. Angiolini *et al.* proposed that chiral properties are due to a chiral helical macromolecular conformation of the polymeric backbone as a consequence of the influence of the stereogenic center on the polymer chain growth. However, the stereogenic center in monomers M8R and M8S is located at the terminal alkyl chain and as a consequence it has a low influence on the polymerization of the methacrylate group. Taking this fact into account, as well as the CD properties of DCM (CD-silent) and DCM/hexane solutions, we propose that the chiral properties are more probably due to a chiral supramolecular organization of chromophores whose handedness is imposed by the molecular chirality.

Chiroptical properties were also evaluated on polymeric films of these polymers. As mentioned above, the mesomorphic behavior of P8S and P8R seems to depend strongly on the thermal history of the sample. For this reason, spectra of these polymers were registered on as-prepared cast films and on thermally treated films—after a slow (1.2 °C/min) and a fast (10 °C/min) cooling process from the isotropic state. UV-Vis spectra of P8S and P8R films were similar to those registered in DCM/hexane solution, which points to similar aggregation behavior (see ESI†). Furthermore, marked differences in the absorption spectra were not observed for polymeric films with different thermal histories. The registered CD spectra of P8S films are presented in Fig. 8 (The ESI includes the CD data for P8R, which are similar to those for P8S but are of opposite sign). These CD spectra are essentially invariable by rotation around the light beam axis, which rules out the existence of linear dichroism in the polymeric films. The CD spectrum of an as-prepared film of P8S

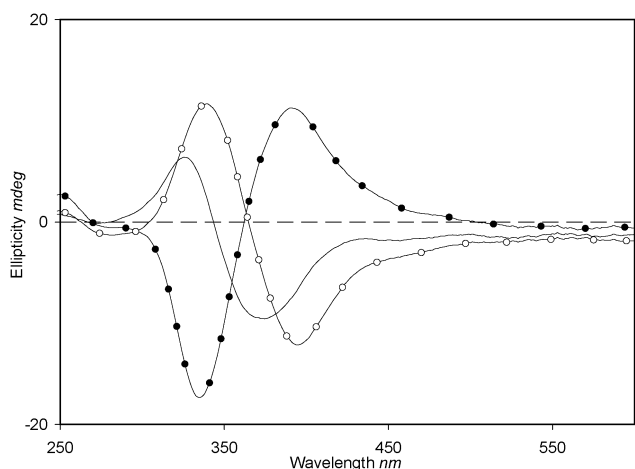


Fig. 8 CD spectra of P8S as prepared film (—), and annealed at isotropic temperature and after cooling down at 10 °C/min (---) and 1.2 °C/min (—●—).

is very similar to that measured in DCM/hexane solution for this polymer (a band corresponding to a negative exciton couplet with a crossover at around 340 nm). However, CD spectra obtained by cooling from the isotropic state to room temperature at different cooling rates depend on the thermal cooling process. The rapidly cooled films exhibit a negative exciton couplet, which is red-shifted with respect to the as-prepared film. Surprisingly, a slow cooling rate (1.2 °C/min) gave rise to a mirror image CD spectrum (a band associated to a positive exciton couplet). This complete stereomutation of the chiral supramolecular organization is caused by the thermal history. Most of the reported examples of stereomutation are due to a change in the surrounding conditions such as solvents, temperature or sample preparation—including cooling rate.^{39–46} In addition, the inversion of chirality in synthetic materials has been found in the field of liquid crystals, specifically those exhibiting chiral mesophases.^{47–49} The observed inversion of the CD spectrum could be due to kinetically and thermodynamically controlled chiral self-organization of azobenzene units with opposite chirality. Taking into account the fact that the configuration of the chiral center in the alkoxy terminal chain is not altered during the stereomutation process, it is required that the two chiral supramolecular forms obtained by slow and fast cooling processes have a diastereomeric relation. Thus, the slow cooling process gives rise to the thermodynamically most stable form, while the fast cooling process freezes the kinetically favored form.

In order to investigate the evolution of the CD response upon thermal treatment, a film of P8S was cooled from the isotropic state to rt at different rates (Fig. 9a). At cooling rates higher or equal to 5 °C/min a negative exciton couplet was detected, the intensity of which decreases with the cooling rate. However, after cooling at 2.5 °C/min the exciton couplet disappears and only a negative Cotton effect at around 340 nm was detected. The inversion of the exciton couplet from negative to positive is clearly induced when the isotropic state is cooled to room temperature at a rate of 1.2 °C/min. According to these results, both diastereomeric supramolecular organizations are probably present in the rapidly cooled materials, but at high cooling rates (≥ 5 °C/min) the kinetically controlled organization is

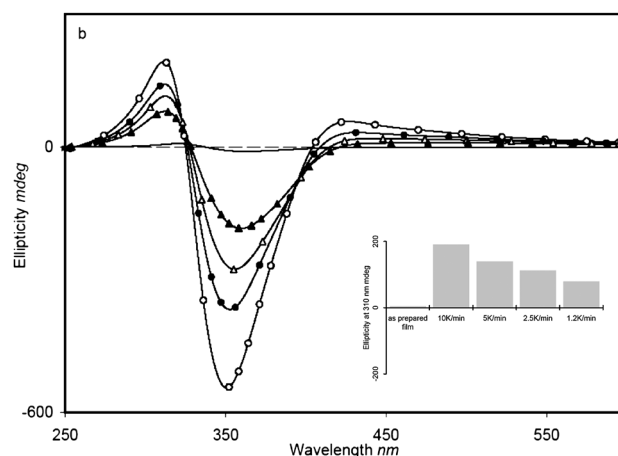
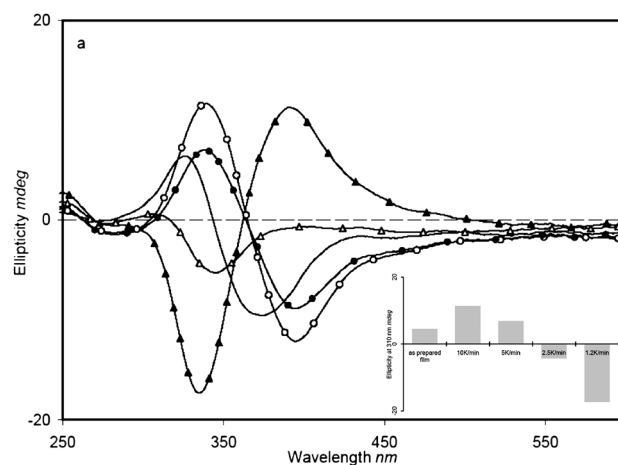


Fig. 9 CD spectra of P8S (a) and P4S/PCN (b): as prepared film (—), and annealed at isotropic temperature after cooling down at 10 °C/min (---); 5 °C/min (—●—); 2.5 °C/min (—△—) and 1.2 °C/min (—▲—). Insets: ellipticity values at 310 nm of P8S (up) and P4S/PCN-25 (down) as prepared film and annealed at isotropic temperature after cooling down at 10 °C/min, 5 °C/min, 2.5 °C/min and 1.2 °C/min.

predominantly obtained. When the cooling rate is 2.5 °C/min the CD signal can correspond to an intermediate of both forms with a slight excess of the thermodynamically controlled form, which clearly prevails at cooling rates equal to or lower than 1.2 °C/min. Furthermore, the stereomutation is detected at a cooling rate similar to that used in the DSC study, which points to a relation between the chiroptical properties and the bistable mesomorphic thermal behavior detected for these polymers.

The CD spectra of copolymers P4S/PCN were also investigated. For these copolymers, as-prepared cast films exhibited an exciton splitting similar to that in P8S with the same thermal history. Annealing of this copolymer in the isotropic state led to an increase in the CD signal, which increases as the cooling rate increases (Fig. 9b). However, stereomutation was not detected for these copolymers, a finding that seems to be in accordance with the observed thermal properties.

Conclusions

A new series of azopolymers having a chiral terminal alkyl chain has been synthesized and characterized. Polymers having a chiral

methylpropyloxy terminal chain exhibit a monolayer smectic A phase but in a very short range of temperature that increases by copolymerization with a cyanoazobenzene monomer. The most interesting results have been obtained for polymers bearing a chiral methylheptyloxy terminal chain (P8S and P8R), which show a bistable mesomorphism governed by the cooling rate from the isotropic state: low cooling rates determine a standard SmA phase and high cooling rates impose a transparent and lamellar mesophase which has been assigned by Kozlovsky and co-workers to a TGBA* phase. Azobenzene units in these azopolymers tend to aggregate both in low polar solvents or in films, which results in chiral supramolecular organizations. The chiroptical properties of the polymeric films strongly depend on the thermal history. Mirror-image CD spectra of P8S (or P8R) are obtained by cooling the films from the isotropic state to rt at different rates. This thermal stereomutation is associated to the bistable mesomorphism. The cooling rate at which mesomorphic and chiroptical properties change, is about 2–5 °C/min. Consequently, these materials have a thermal and reversible switching both on mesomorphic and chiroptical properties.

Acknowledgements

This work was supported by the MICINN, Spain, under the project MAT2008-06522-C02 and FEDER fundings. J. del Barrio acknowledges his grant from DGA (Government of Aragón).

References

- H. Kitzerow and C. Bahr, *Chirality in Liquid Crystals*, Springer-Verlag, New York, 2001.
- J. M. Ribo, J. Crusats, F. Sagues, J. Claret and R. Rubires, *Science*, 2001, **292**, 2063–2066.
- T. Yamaguchi, T. Kimura, H. Matsuda and T. Aida, *Angew. Chem. Int. Ed.*, 2004, **43**, 6350–6355.
- H. Rau, *Chiral Photochemistry*, Marcel Dekker, New York, 2004.
- A. Natansohn and P. Rochon, *Chem. Rev.*, 2002, **102**, 4139–4175.
- T. Ikeda, J.-i. Mamiya and Y. Yu, *Angew. Chem. Int. Ed.*, 2007, **46**, 506–528.
- A. S. Matharu, S. Jeeva and P. P. Ramanujan, *Chem. Soc. Rev.*, 2007, **36**, 1868–1880.
- S.-W. Choi, T. Izumi, Y. Hoshino, Y. Takanishi, K. Ishikawa, J. Watanabe and H. Takezoe, *Angew. Chem. Int. Ed.*, 2006, **45**, 1382–1385.
- F. Vera, R. M. Tejedor, P. Romero, J. Barbera, M. B. Ros, J. L. Serrano and T. Sierra, *Angew. Chem. Int. Ed.*, 2007, **46**, 1873–1877.
- L. Nikolova, T. Todorov, M. Ivanov, F. Andruzzi, S. Hvilsted and P. S. Ramanujam, *Opt. Mater.*, 1997, **8**, 255–258.
- G. Iftime, F. L. Labarthe, A. Natansohn and P. Rochon, *J. Am. Chem. Soc.*, 2000, **122**, 12646–12650.
- L. Nedelchev, A. Matharu, L. Nikolova, S. Hvilsted and P. S. Ramanujam, *Mol. Cryst. Liq. Cryst.*, 2002, **375**, 563–575.
- G. Cipparrone, P. Pagliusi, C. Provenzano and V. P. Shibaev, *Macromolecules*, 2008, **41**, 5992–5996.
- R. M. Tejedor, M. Millaruelo, L. Oriol, J. L. Serrano, R. Alcalá, F. J. Rodriguez and B. Villacampa, *J. Mater. Chem.*, 2006, **16**, 1674–1680.
- R. M. Tejedor, L. Oriol, J. L. Serrano, F. Partal Ureña and J. J. López González, *Adv. Func. Mater.*, 2007, **17**, 3486–3492.
- A. Bobrovsky, V. P. Shibaev and J. Wendorff, *Liq. Cryst.*, 2007, **34**, 1–7.
- L. M. Blinov, M. V. Kozlovsky, M. Ozaki, K. Skarp and K. Yoshino, *J. Appl. Phys.*, 1998, **84**, 3860–3866.
- D. Kilian, M. Kozlovsky and W. Haase, *Liq. Cryst.*, 1999, **26**, 705–708.
- M. V. Kozlovsky, V. P. Shibaev, A. I. Stakhanov, T. Weyrauch and W. Haase, *Liq. Cryst.*, 1998, **24**, 759–767.
- M. Kozlovsky and V. V. Lazarev, *Macromol. Rapid Comm.*, 2006, **27**, 361–365.
- A. V. Medvedev, E. B. Barmatov, A. S. Medvedev, V. P. Shibaev, S. A. Ivanov, M. Kozlovsky and J. Stumpe, *Macromolecules*, 2005, **38**, 2223–2229.
- V. R. I. B. E. R. M. K. Sergey Polushin, *Macromol. Rapid Comm.*, 2008, **29**, 224–228.
- Z. Zheng, Y. Y. Sun, J. Xu, B. Chen, Z. Q. Su and Q. J. Zhang, *Polym. Int.*, 2007, **56**, 699–706.
- Z. Zheng, J. Xu, Y. Sun, J. Zhou, B. Chen, Q. Zhang and K. Wang, *J. Polym. Sci., Part A: Polym. Chem.*, 2006, **44**, 3210–3219.
- L. Angiolini, T. Benelli, R. Bozio, A. Daurù, L. Giorgini and D. Pedron, *Synth. Met.*, 2003, **139**, 743–746.
- L. Angiolini, R. Bozio, L. Giorgini, D. Pedron, G. Turco and A. Daurù, *Chem. Eur. J.*, 2002, **8**, 4241–4247.
- L. Angiolini, D. Caretti, L. Giorgini, E. Salatelli, A. A. C. Carlini and R. Solaro, *Polymer*, 1998, **39**, 6621–6629.
- L. Angiolini, L. Giorgini, R. Bozio and D. Pedron, *Synth. Met.*, 2003, **138**, 375–379.
- V. P. Shibaev and N. A. Plate, *Pure Appl. Chem.*, 1985, **57**, 1589–1602.
- G. Odian, *Principles of Polymerization*, Wiley-Interscience, Hoboken, 2004.
- L. Mandelkern, *Crystallization of Polymers*, McGraw-Hill, New York, 1964.
- M. Kozlovsky, B. J. Jungnickel and H. Ehrenberg, *Macromolecules*, 2005, **38**, 2729–2738.
- L. Bata, K. Fodorcsorba, J. Szabon, M. V. Kozlovsky and S. Holly, *Ferroelectrics*, 1991, **122**, 149–158.
- I. Dierking and S. T. Lagerwall, *Liq. Cryst.*, 1999, **26**, 83–95.
- R. M. Tejedor, L. Oriol, J. L. Serrano and T. Sierra, *J. Mater. Chem.*, 2008, **18**, 2899–2908.
- M. Shimomura, R. Ando and T. Kunitake, *Ber. Bunsenges. Phys. Chem.*, 1983, **87**, 1134–1143.
- L. Angiolini, D. Caretti, L. Giorgini and E. Salatelli, *Polymer*, 2001, **42**, 4005–4016.
- A. Painelli, F. Terenziani, L. Angiolini, T. Benelli and L. Giorgini, *Chem. Eur. J.*, 2005, **11**, 6053–6063.
- G. Bidan, S. Guillerez and V. Sorokin, *Adv. Mater.*, 1996, **8**, 157–160.
- M. M. Bouman and E. W. Meijer, *Adv. Mater.*, 1995, **7**, 385–387.
- K. Hayakawa, M. Sato, I. Nagata, N. Yamato, H. Murata and M. Tanokura, *Colloid & Polymer Science*, 2006, **284**, 1453–1458.
- A. Lohr, M. Lysetska and F. Würthner, *Angew. Chem. Int. Ed.*, 2005, **44**, 5071–5074.
- J. Ma, H. S. Cheon and Y. Kishi, *Org. Lett.*, 2007, **9**, 319–322.
- H. Nakashima, M. Fujiki, J. R. Koe and M. Motonaga, *J. Am. Chem. Soc.*, 2001, **123**, 1963–1969.
- X. D. Song, J. Perlstein and D. G. Whitten, *J. Am. Chem. Soc.*, 1997, **119**, 9144–9159.
- T. Fukushima, K. Takachi and K. Tsuchihara, *Macromolecules*, 2008, **41**, 6599–6601.
- A. V. Emelyanenko, M. A. Osipov and D. A. Dunmur, *Phys. Rev. E*, 2000, **62**, 2340–2352.
- C. Loubser, P. L. Wessels, P. Styring and J. W. Goodby, *J. Mater. Chem.*, 1994, **4**, 71–79.
- T. Kato, T. Matsuoka, M. Nishii, Y. Kamikawa, K. Kanie, T. Nishimura, E. Yashima and S. Ujiie, *Angew. Chem. Int. Ed.*, 2004, **43**, 1969–1972.